J|A|C|S
ARTICLES
Published on Web 02/10/2004

Nucleophilic Participation in the Transition State for Human Thymidine Phosphorylase

Matthew R. Birck and Vern L. Schramm*

Contribution from the Department of Biochemistry, Albert Einstein College of Medicine, 1300 Morris Park Avenue Bronx, New York 10461

Received October 27, 2003; E-mail: vern@aecom.yu.edu

Abstract: Recombinant human thymidine phosphorylase catalyzes the reaction of arsenate with thymidine to form thymine and 2-deoxyribose 1-arsenate, which rapidly decomposes to 2-deoxyribose and inorganic arsenate. The transition-state structure of this reaction was determined using kinetic isotope effect analysis followed by computer modeling. Experimental kinetic isotope effects were determined at physiological pH and 37 °C. The extent of forward commitment to catalysis was determined by pulse-chase experiments to be 0.70%. The intrinsic kinetic isotope effects for [1′-^{3}H]-, [2′*R*-^{3}H]-, [2′*S*-^{3}H]-, [4′-^{3}H]-, [5′-^{3}H]-, [1′-^{14}C]-, and [1-^{15}N]-thymidines were determined to be 0.989 ± 0.002, 0.974 ± 0.002, 1.036 ± 0.002, 1.020 ± 0.003, 1.061 ± 0.003, 1.139 ± 0.005, and 1.022 ± 0.005, respectively. A computer-generated model, based on density functional electronic structure calculations, was fit to the experimental isotope effect. The structure of the transition state confirms that human thymidine phosphorylase proceeds through an S_N2-like transition state with bond orders of 0.50 to the thymine leaving group and 0.33 to the attacking oxygen nucleophile. The reaction differs from the dissociative transition states previously reported for *N*-ribosyl transferases and is the first demonstration of a nucleophilic transition state for an *N*-ribosyl transferase. The large primary ^{14}C isotope effect of 1.139 can occur only in nucleophilic displacements and is the largest ^{14}C primary isotope effect reported for an enzymatic reaction. A transition state structure with substantial bond order to the attacking nucleophile and leaving group is confirmed by the slightly inverse 1′-^{3}H isotope effect, demonstrating that the transition state is compressed by the impinging steric bulk of the nucleophile and leaving group.

Introduction

Platelet-derived endothelial cell growth factor (PD-ECGF) is involved in angiogenesis and chemotaxis in human solid tumors[1−3] and in suppression of hypoxia-induced apoptosis.[4−6] Cellular expression of PD-ECGF correlates well with the aggressiveness and invasiveness of human cancers, including colon, esophageal, gastric, breast, bladder, ovarian, and lung primary malignancies.[7−14] Thymidine phosphorylase (TP) is a highly specific *N*-ribosyl phosphorylase,[15−19] catalyzing the phosphorolysis of 2′-deoxypyrimidine nucleosides. The sequencing of PD-ECGF by Moghaddam and Bicknell[20] revealed that PD-ECGF is the enzyme TP. Angiogenesis is caused by 2-deoxyribose, formed by dephosphorylation of 2-deoxyribose 1-phosphate, the product of the TP reaction.[21−24]

(1) Ishikawa, F.; Miyazono, K.; Hellman, U.; Drexler, H.; Wernstedt, C.; Usuki, K.; Takaku, F.; Risau, W.; Heldin, C.-H. *Nature* **1989**, *338*, 557−562.
(2) Furukawa, T.; Yoshimura, A.; Sumizawa, T.; Haraguchi, M.; Akiyama, S.-I.; Fukui, K.; Ishizawa, M.; Yamada, Y. *Nature (London)* **1992**, *356*, 668−.
(3) Haraguchi, M.; Miyadera, K.; Uemura, K.; Sumizawa, T.; Furukawa, T.; Yamada, K.; Akiyama, S.; Yamada, Y. *Nature* **1994**, *368*, 198.
(4) Matshushita, S.; Nitanda, T.; Furukawa, T.; Sumizawa, T.; Tani, A.; Nishimoto, K.; Akiba, S.; Miyadera, K.; Fukushima, M.; Yamada, Y.; Yoshida, H.; Kanzaki, T.; Akiyama, S. *Cancer Res.* **1999**, *59*, 1911−1916.
(5) Kitazono, M.; Takebayashi, Y.; Ishitsuka, K.; Takao, S.; Tani, A.; Furukawa, T.; Miyadera, K.; Yamada, Y.; Aikou, T.; Akiyama, S. *Biochem. Biophys. Res. Commun.* **1998**, *253*, 797−803.
(6) Ikeda, R.; Furukawa, T.; Kitazono, M.; Ishitsuka, K.; Okumura, H.; Tani, A.; Sumizawa, T.; Haraguchi, M.; Komatsu, M.; Uchimiya, H.; Ren, X. Q.; Motoya, T.; Yamada, K.; Akiyama, S. *Biochem. Biophys. Res. Commun.* **2002**, *291*, 806−812.
(7) Saeki, T.; Tanada, M.; Takashima, S.; Saeki, H.; Takiyama, W.; Nishimoto, N.; Moriwaki, S. *Jpn. J. Clin. Oncol.* **1997**, *27*, 227−230.
(8) Relf, M.; LeJeune, S.; Scott, P. A.; Fox, S.; Smith, K.; Leek, R.; Moghaddam, A.; Whitehouse, R.; Bicknell, R.; Harris, A. L. *Cancer Res.* **1997**, *57*, 963−969.
(9) Giatromanolaki, A.; Koukourakis, M. I.; Comley, M.; Kaklamanis, L.; Turley, H.; O'Byrne, K.; Harris, A. L.; Gatter, K. C. *J. Pathol.* **1997**, *181*, 196−199.
(10) Takebayashi, Y.; Natsugoe, S.; Baba, M.; Akiba, S.; Fukumoto, T.; Miyadera, K.; Yamada, Y.; Takao, S.; Akiyama, S.; Aikou, T. *Cancer* **1999**, *85*, 282−289.
(11) Tokunaga, Y.; Hosogi, H.; Hoppou, T.; Nakagami, M.; Tokuka, A.; Ohsumi, K. *Surgery* **2002**, *131*, 541−547.
(12) Shimada, H.; Takeda, A.; Shiratori, T.; Nabeya, Y.; Okazumi, S.; Matsubara, H.; Funami, Y.; Hayashi, H.; Gunji, Y.; Kobayashi, S.; Suzuki, T.; Ochiai, T. *Cancer* **2002**, *94*, 1947−1954.
(13) Miyadera, K.; Sumizawa, T.; Haraguchi, M.; Yoshida, H.; Konstanty, W.; Yamada, Y.; Akiyama, S. *Cancer Res.* **1995**, *55*, 1687−1690.
(14) Takao, S.; Takebayashi, Y.; Che, X.; Shinchi, H.; Natsugoe, S.; Miyadera, K.; Yamada, Y.; Akiyama, S.; Aikou, T. *Clin. Cancer Res.* **1944**, *4*, 1619−1624.
(15) Manson, L. A. In September 1948 Meeting of the American Chemical Society.
(16) Manson, L. A.; Lampen, J. O. *Fed. Proc.* **1949**, 8.
(17) Razzell, W. E.; Khorana, H. G. *Biochim. Biophys. Acta* **1958**, *28*, 562−566.
(18) Nakayama, C.; Wataya, Y.; Rich B. Meyer, J.; Santi, D. V.; Saneyoshi, M.; Ueda, T. *J. Med. Chem.* **1980**, *23*, 962−964.
(19) Avraham, Y.; Grossowicz, N.; Yashphe, J. *Biochim. Biophys. Acta* **1990**, *1040*, 287−293.
(20) Moghaddam, A.; Bicknell, R. *Biochemistry* **1992**, *31*, 12141−12146.
(21) Hotchkiss, K. A.; Ashton, A. W.; Schwartz, E. L. *J. Biol. Chem.* **2003**, *278*, 19272−19279.
(22) Hotchkiss, K. A.; Ashton, A. W.; Klein, R. S.; Lenzi, M. L.; Shu, G. H.; Schwartz, E. L. *Cancer Res.* **2003**, *63*, 527−533.
(23) de Bruin, M.; Smid, K.; Laan, A. C.; Noordhuis, P.; Fukushima, M.; Hoekman, K.; Pinedo, H. M.; Peters, G. J. *Biochem. Biophys. Res. Commun.* **2003**, *301*, 675−679.

Table 1. Thymidines Specifically Synthesized with Radiolabels and the Respective KIEs

product thymidine	starting material	remote label	experimental KIE
[1′-^{3}H]dT	[2-^{3}H]glucose	[5′-^{14}C]dT	α-secondary ^{3}H
[2′*R*-^{3}H]dT	[2′*R*-^{3}H]dATP	[5′-^{14}C]dT	β-(*R*)-secondary ^{3}H
[2′*S*-^{3}H]dT	[2-^{3}H]ribose 5-phosphate	[5′-^{14}C]dT	β-(*S*)-secondary ^{3}H
[4′-^{3}H]dT	[5-^{3}H]glucose	[5′-^{14}C]dT	remote secondary ^{3}H
[5′-^{3}H]dT	Commercially available	[5′-^{14}C]dT	remote secondary ^{3}H
[1′-^{14}C]dT	[2-^{14}C]glucose	[4′-^{3}H]dT	primary ^{14}C
[5′-^{14}C]dT	[6-^{14}C]glucose	n.a.[a]	remote secondary ^{14}C
[1-^{15}N]dT	[1-^{15}N]thymine	n.a.[b]	primary ^{15}N

[a] The KIE of [5′-^{14}C]dT is assumed to be unity. [b] KIE [1-^{15}N]dT is determined using mass-spectroscopy.

Inhibition of TP is postulated to slow tumor growth and metastasis by decreasing the nutrient oxygen supply to cancerous cells.[25] Although inhibitors have been reported that are purported to resemble the putative transition state of TP, the structure of the transition state is hypothetical and is based on the known transition-state structures of purine nucleoside phosphorylase (PNP),[26] AMP nucleosidase,[27] and uracil-DNA glycosylase.[28] These enzymes are known to proceed through transition states characterized by highly dissociated leaving groups, significant oxacarbenium ion character, and little nucleophilic participation.

Transition-state analysis of *N*-ribosyl transferases has become well developed through analysis of kinetic isotope effects (KIE). Multiple KIEs are measured at positions close to the C−N ribosidic bond. The KIEs are used to constrain a computational model of the transition state consistent with the experimental KIEs. This transition-state structure can serve as a blueprint for the design of stable analogues with molecular electrostatic potential surfaces similar to the enzyme-stabilized transition state.[29]

Knowledge of the transition-state structure has the potential to lead to more potent inhibitors, hence, more efficacious inhibition of TP. Potential biological uses of TP inhibitors include the above-mentioned antiangiogenesis, but inhibitors could also find use in blocking TP in its role of inactivating 2′-deoxy-5-fluorouridine (5FdU), both a clinically used antineoplastic and a product of 5-fluorouracil metabolism. It is the precursor to 5FdU-5′-phosphate, a covalent inactivator of thymidylate synthetase.[30,31] Overexpression of TP correlates both with decreased efficacy of 5FdU[32,33] and, in some cancer cell lines, increased efficacy of 5-fluorouracil.[25] Thus the inhibition of TP should have the opposite effect, decreased metabolism of the 5FU pathway and decreased deactivation of 5FdU. The combination of powerful TP inhibitors with thymidylate synthetase antimetabolite precursors, such as 5FdU or 2′-deoxy-5-(trifluoromethyl)uridine, may provide improved synergistic therapies.[34]

Methods and Materials

Preparation of TP. Recombinant human thymidine phosphorylase was provided by Dr. Paula Krosky at the National Institutes of Health from *Escherichia coli* BL21(DE3) cells transformed with the pCal-*n*-EK/TP (pCal-*n*-EK from Invitrogen) and pGroESL vectors. Purification was performed on a calmodulin column, and the calmodulin binding protein was cleaved from TP using enterokinase, which was removed using soybean trypsin inhibitor−sepharose. TP was concentrated to approximately 3 mg/mL and stored at −70 °C.

Isotopically Labeled ATP. ATPs labeled specifically with ^{3}H, ^{14}C, and ^{15}N were synthesized from radiolabeled glucose and ribose-5-phosphate using a method similar to that described by Parkin et al.[35,36] in reaction mixtures containing 3 mM adenine, 135 mM KPO_4, 50 mM glycylglycine (pH = 7.4), 50 mM KCl, 50 mM $MgCl_2$, 5 mM NH_4Cl, 2 mM glucose, 2.5 mM DTT, 20 mM α-ketoglutarate, 100 μM $NADP^+$, 200 mM phospho*enol*pyruvate, and 400 μM ATP in addition to the radiolabeled substrate (Table 1). Enzymes were prepared by centrifugation to remove excess $(NH_4)_2SO_4$. The reaction was initiated by the addition of: phosphoribose isomerase (1−10 units), pyruvate kinase (2 units), glutamate dehydrogenase (0.5 unit), glucose-6-phosphate dehydrogenase (0.5 unit), 6-phosphogluconate dehydrogenase (1 unit), adenylate kinase (4 units), adenine phosphoribosyltransferase (1 unit), phosphoribosyl pyrophosphate synthase (1 unit), and hexokinase (0.5 unit) (added last). The reaction mixture was incubated at 37 °C and the reaction monitored for adenine and ATP by HPLC. ATPs were purified by reverse phase HPLC (C-18 Deltapak column, 50 mM ammonium formate pH 4.1, 1 mL/min) and lyophilized. Yields were approximately 85% by radiolabel incorporation from glucose into ATP.

Isotopically Labeled dATP. Reduction of ATP to dATP was accomplished with ribonucleotide triphosphate reductase (50 mM phosphate pH 6.8, 100 mM DTT, 1 M NaOAc, 2 mM $CaCl_2$, 100 μM cobalamin in a total of 5 mL). The ribonucleotide triphosphate reductase reaction was carried out at 37 °C in the dark for 2−4 h. The resulting dATP was purified by HPLC as described for ATP with the addition of 10% MeOH to the mobile phase. Yields averaged 65% by HPLC analysis.

Isotopically Labeled thymidine. Thymidine (dT) was synthesized from dATP in two steps (Figure 1). First, dATP was converted into 2′-deoxyinosine through the action of hexokinase, adenylate kinase, alkaline phosphatase, and adenosine deaminase in 50 mM HEPES, pH 7.4. Conversion was quantitative by HPLC. These enzymes were inactivated by immersion in a 100 °C water bath for 5 min. The solution was cooled and the remaining enzymes, PNP and TP, were added at 37 °C, along with 1 mM thymine, and the reaction was allowed to proceed to equilibrium. A PNP/TP ratio of ∼1/10 and excess of thymine resulted in >90% yield of thymidine. For synthesis of [1-^{15}N]dT, ribose

(24) Sengupta, S.; Sellers, L. A.; Matheson, H. B.; Fan, T. P. *Br. J. Pharmacol.* **2003**, *139*, 219−231.
(25) Focher, F.; Spadari, S. *Curr. Cancer Drug Targets* **2001**, *1*, 141−153.
(26) Kline, P. C.; Schramm, V. L. *Biochemistry* **1993**, *32*, 13212−13219.
(27) Mentch, F.; Parkin, D. W.; Schramm, V. L. *Biochemistry* **1987**, *26*, 921−930.
(28) Werner, R. M.; Stivers, J. T. *Biochemistry* **2000**, *39*, 14054−14064.
(29) Schramm, V. L.; Horenstein, B. A.; Bagdassarian, C. K.; Schwartz, S. D.; Berti, P. J.; Rising, K. A.; Scheuring, J.; Kline, P. C.; Parkin, D. W.; Merkler, D. J. *Journal of Quantum Chemistry: Quantum Biology Symposium* **1996**, *23*, 1805−1813.
(30) Santi, D. V.; McHenry, C. S.; Raines, R. T.; Ivanetich, K. M. *Biochemistry* **1987**, *26*, 8606−8613.
(31) Santi, D. V.; McHenry, C. S.; Sommer, H. *Biochemistry* **1974**, *13*, 3.
(32) Foth, H.; Hellkamp, J.; Kunellis, E.-M.; Kahl, G. F. *Drug Metab. Dispos.* **1990**, *18*, 1011−1017.
(33) Patterson, A. V.; Zhang, H. T.; Moghaddam, A.; Bicknell, R.; Talbot, D. C.; Stratford, I. J.; Harris, A. L. *Br. J. Cancer* **1995**, *72*, 669−675.
(34) de Bruin, M.; van Capel, T.; Van der Born, K.; Kruyt, F. A.; Fukushima, M.; Hoekman, K.; Pinedo, H. M.; Peters, G. J. *Br. J. Cancer* **2003**, *88*, 957−964.
(35) Parkin, D. W.; Leung, H. B.; Schramm, V. L. *J. Biol. Chem.* **1984**, *259*, 9411−9417.
(36) Parkin, D. W.; Schramm, V. L. *Biochemistry* **1987**, *26*, 913−920.

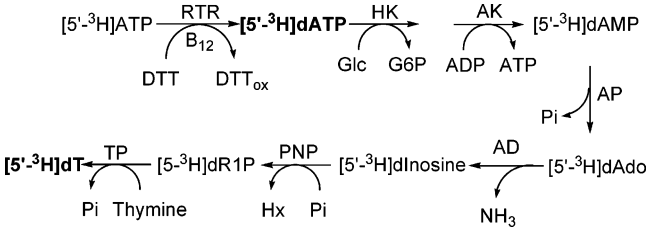

Figure 1. Synthetic route for production of radiolabeled dT beginning with the appropriately labeled ATP. Synthesis of ATP can be found in Parkin and Schramm.[35,36] Those compounds labeled in boldface type were purified by HPLC. Abbreviations used: AD, adenosine deaminase; AK, adenylate kinase; AP, alkaline phosphatase; B_{12}, adenosyl cobalamine; dR1P, 2-deoxyribose 1-phosphate; dT, thymidine; HK, hexokinase; RTR, ribonucleotide triphosphate reductase.

1-phosphate (Sigma) was in 5-fold excess over [1-^{15}N]thymine, a generous gift of Industrial Research, Ltd. (Lower Hutt, New Zealand), and only TP was added. Thymidine was purified by HPLC (as for ATP with the addition of 10% MeOH). The radiolabeled thymidines were concentrated and stored at −20 °C. Yields were generally above 90% for the final reaction step and were 50−60% overall from labeled glucoses.

[5′-^{3}H]dT was purchased from Moravek, Inc. or American Radiolabeled Chemicals, Inc. and repurified by HPLC as above before use.

Determination of KIEs by Scintillation Counting. KIEs were determined by a method similar to that previously described by this laboratory.[35] Two radiolabeled thymidines were mixed as described in Table 1 at a ratio of at least 3:1 for ^{3}H:^{14}C to facilitate resolution of the of the β-emission spectra. Each assay was performed in a total of 1 mL (50 mM HEPES pH 7.4, 5 mM $NaAsO_4$, 50 μM carrier thymidine, 11 nM TP) with at least 10^5 cpm ^{14}C. Reactions were allowed to proceed to 20−25% completion and split into three parts. One aliquot was allowed to react to 100% completion, while the other two were stopped. Samples were applied to a charcoal spin-column (100 mg of activated charcoal in a Qiagen DNA purification spin column, previously washed with 1 mL of 10 mM 2-deoxyribose (2-dRib) in 10% ethanol) and eluted with 3 mL of 10 mM 2-dRib in 10% ethanol. The eluted fractions were mixed with scintillation fluid (7 mL, National Diagnostics Liquiscint) for a total of 10 mL and counted for at least five cycles at 10 min per cycle.

The count rate was averaged over all cycles, and the ^{3}H and ^{14}C emissions were separated according to the spectra of standard ^{14}C samples in identical matrixes according to eqs 1 and 2, where "^{14}C channel ratio" is the ratio of ^{14}C counts in channels A and B for a control compound, [1-^{14}C]glucose. The spectral windows are set such that no counts from ^{3}H appear in channel B.

$$\text{cpm}(^3\text{H}) = \text{cpm}_{\text{channel}A} - \text{cpm}_{\text{channel}B} \times (^{14}\text{C channel ratio}) \quad (1)$$

$$\text{cpm}(^{14}\text{C}) = \text{cpm}_{\text{channel}B} + \text{cpm}_{\text{channel}B} \times (^{14}\text{C channel ratio}) \quad (2)$$

The ratios of ^{3}H to ^{14}C were determined for both the 20−25% reactions and the 100% reaction and the KIEs, adjusted to 0% reaction, were calculated according to eq 3,

$$\text{KIE} = \frac{\ln\left[\dfrac{1 - f\left(\dfrac{\text{light}}{\text{heavy}}\right)_{\text{partial}}}{\left(\dfrac{\text{light}}{\text{heavy}}\right)_{\text{complete}}}\right]}{\ln(1 - f)} \quad (3)$$

where f is the fraction of reaction progress as determined by HPLC and "light and heavy" are the corrected cpm values for the remotely labeled compound and the compound of interest, respectively.

Determination of KIEs by Electrospray Ionization Mass Spectrometry. [1-^{15}N]dT and natural abundance thymidine were mixed in approximately equal amounts. The enzymatic reaction was performed exactly as described above except that no carrier thymidine was added. Before addition of TP, 200 μL of reaction mixture was removed for separate analysis. At 20−30% completion, the remaining 800 μL of the reaction mixture was quenched by heating at 100 °C for 5 min. This was then split into two 400-μL fractions for a total of three aliquots. Thymidine and, in the partial reaction mixtures, thymine were separated by HPLC (0.1% formic acid and 10% MeOH on a 300-mm DeltaPak reverse phase column at 1 mL/min). ESI TOF-MS was performed on the Mariner API-TOF mass spectrometer (Applied Biosystems, CA). Samples were infused at 5 μL/min and 50 scans from 100 to 500 *m*/*z* were averaged to determine the areas of the thymine and thymidine peaks. The ratios of unlabeled/labeled for both thymine and thymidine were determined for the pure [1-^{15}N]dT, natural abundance thymidine, the 0% conversion sample, and both 20−30% conversion samples. In the experimental samples, the ratios were corrected for the natural abundance of the heavy isotope peak in the unenriched dT, and the KIE was calculated.[37]

Table 2. Experimental and Intrinsic KIEs Compared to Those Calculated for the Model Transition State

position	experimental KIE	model KIE[a]
1′-^{3}H	0.989 ± 0.002 (9)[b]	0.981
1′-^{14}C	1.139 ± 0.005 (5)	1.144
2′*R*-^{3}H	0.974 ± 0.002 (8)	0.941
2′*S*-^{3}H	1.036 ± 0.002 (6)	1.026
4′-^{3}H	1.020 ± 0.003 (6)	1.046
5′-^{3}H	1.061 ± 0.003 (3)	1.066[c]
5′-^{14}C	1.000[d]	1.001
1-^{15}N	1.022 ± 0.005 (2)	1.012

[a] Model KIE was calculated using Isoeff98 from frequencies determined for the substrate and transition state at B1LYP/6-31G*. [b] Number in parentheses refers to the number of trials. [c] Average of pro*R* and pro*S* positions. [d] Assumed to be unity.

Due to the low commitment to catalysis (see below), the experimental KIEs are considered to be equal to the intrinsic KIEs. In the case of [1′-^{14}C]dT, the KIE observed was corrected for the KIE of the remote label, [4′-^{3}H]dT, to give the intrinsic KIE (Table 2).

Commitment to Catalysis. The isotope-trapping method was used to determine commitment to catalysis. In a total of 25 μL, 50 mM HEPES (pH 7.4), 23 μM TP, and 500 μM thymidine containing approximately 10^5 cpm [5′-^{3}H]dT were mixed and allowed to equilibrate at 37 °C for 6 s. Five hundred μL of a chase solution (equilibrated to 37 °C) containing 50 mM HEPES (pH 7.4), 1 mM unlabeled thymidine, and varying concentrations of sodium arsenate (10 μM, 50 μM, 500 μM, 1 mM, 5 mM) were added, and the reaction was allowed to proceed for approximately 20 catalytic cycles. Control reactions were performed with the chase solution added before the enzyme, and the reaction was allowed to proceed for the same length of time. Reactions were quenched by freezing at −72 °C in a dry ice−ethanol bath. 2-Deoxyribose generated in the reaction was quantitated by thawing samples on ice and immediately applying them to charcoal spin columns as described above. The commitment factor was determined by plotting $1/([\text{dT}]_{\text{trapped}}/[\text{TP}]_{\text{total}})$ versus $1/[\text{AsO}_4]$. The *y*-intercept represents the concentration of thymidine trapped by TP at infinite substrate concentration (Figure 2).

Modeling of Transition State. An in vacuo transition state[38] was determined at the density functional level (B1LYP/6-31G*) using Gaussian98's implementation of the synchronous transit-guided quasi-Newton method, using thymidine and dianionic phosphate[39] as starting materials and deprotonated thymine and ribose 1-phosphate as prod-

(37) Berti, P. J.; Blanke, S. R.; Schramm, V. L. *J. Am. Chem. Soc.* **1997**, *119*, 12079−12088.
(38) The calculated TS, along with frequency tables and, where appropriate, calculated KIEs are included in the Supporting Information.
(39) Electron density at the attacking oxygen of dianionic phosphate and arsenate differ by 0.02. This alters the nucleophile/leaving group distances by less than 0.05 Å.

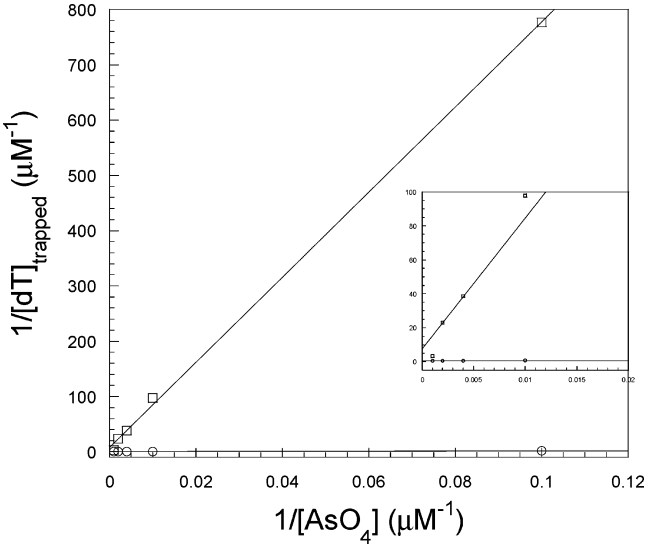

Figure 2. Commitment to catalysis of human TP using 23 μM TP (20.8 μM bound). (Inset) Closeup view of the intersection of the control and experimental lines with the *y*-axis. In both, (□) represents experimental data while (○) denotes control data. The *y*-intercept of 7.66 μM^{-1} corresponds to a forward commitment to catalysis of 0.7%.

ucts.[40] The isotope effects for this model transition state were determined using Isoeff98.[41] Constraints were applied to the distance between C1′−N1 and/or C1′−O (phosphate), and the calculated transition state was reoptimized using the Berny algorithm.[40,42] All constraints were released prior to the frequency calculations in those models where constraints were used. Isotope effects were then recalculated and compared to their experimental values. The constraints were altered, and the process was repeated until the KIEs predicted by the transition-state model were a good match to the experimental KIEs.

Results and Discussion

Commitment to Catalysis. Commitment to catalysis was defined by Northrop[43] as

$$^3(V/K) = \frac{^3k + c_f + c_r{}^3K_{eq}}{1 + c_f + c_r} \quad (4)$$

where $^3(V/K)$ is the observed tritium KIE, ^3k is the intrinsic KIE, c_f is the forward commitment, c_r is the reverse commitment, and $^3K_{eq}$ is the equilibrium isotope effect.

Intrinsic KIEs are difficult to measure in freely reversible enzymatic reactions with both forward and reverse commitments.[43] Therefore, arsenate was used instead of phosphate as the attacking nucleophile to eliminate the reverse reaction. The product of arsenolysis, 2-deoxyribose 1-arsenate, is chemically unstable and hydrolyzes, via water attack on the arsenic,[26] to form 2-dRib and inorganic arsenate,[44] preventing reformation of thymidine and rendering the TP reaction irreversible following release of 2-deoxyribose 1-arsenate into solution. Although we cannot fully eliminate the possibility of reverse commitment due to on-enzyme reversibility, it must be less than 4.5% to avoid an intrinsic 1′-^{14}C KIE above the theoretical maximum of approximately 1.145. This places the KIE measured here near the maximum possible, making the reverse commitment insignificant and reducing eq 4 to

$$^3(V/K) = \frac{^3k + c_f}{1 + c_f} \quad (5)$$

Forward commitment to catalysis can also mask KIEs in many systems.[43] Forward commitment defines the tendency of the Michaelis complex either to proceed forward to product or to release substrates back into solution. Trapping experiments, similar to those described by Rose,[45] were performed at 23 μM TP and 500 μM thymidine, giving 20.8 μM bound enzyme (90.2%). Extrapolation of the resulting line (Figure 2) to zero arsenate gives a concentration of 130 nM trapped thymidine. This corresponds to a forward commitment to catalysis of 0.7% for the arsenolysis reaction (Figure 2). Low forward commitment establishes that the binding of thymidine to TP has a low energy barrier relative to the chemical step(s). This result is consistent with the relatively high K_m (54 μM) and low k_{cat} (2 s^{-1}) for the assay conditions used here. Correcting the experimental KIE for the measured commitment to catalysis does not change the value of the KIE within experimental error; thus, the experimental KIEs can be considered intrinsic.

Primary [1′-^{14}C]dT KIE. Intrinsic KIE values for human TP differ from those observed for other *N*-ribosyl transferase reactions. The large primary 1′-^{14}C and slightly inverse α-secondary 1′-^{3}H KIEs readily establish that the arsenolysis of thymidine by TP proceeds via an associative, S_N2-like TS, similar to that of *S*-adenosylmethionine (SAM) synthetase.[46] In PNP,[26] pertussis (PTA),[47] diphtheria (DTA),[37] and cholera (CTA) toxins,[48] the transition states are S_N1-like with significant oxacarbenium ion character. Ricin A-chain (RTA)[49] and uracil-DNA glycosylase,[28] which deadenylate and deuridinylate RNA and DNA, respectively, proceed through completely dissociative reactions with fully developed ribooxacarbenium ions.[50] Primary ^{14}C KIEs for these S_N1 reactions vary from 1.015 for ricin A-chain to 1.049 for the ADP-ribosylation of $G_{i\alpha1}$ by pertussis toxin.

Primary ^{14}C KIEs are widely used to differentiate between S_N1 and S_N2 reaction mechanisms. The primary ^{14}C KIE is dependent on the symmetry of nucleophilic participation at the transition state, the change in bond order at the carbon center, and reaction coordinate motion of the carbon. High primary ^{14}C KIEs (>9%) indicate significant bond orders to both the C−leaving group and C−nucleophile bonds, characteristic of an S_N2 transition state. Small primary ^{14}C KIEs demonstrate small bond orders from the nucleophile and leaving group and small reaction coordinate motion at the primary C in the transition state. These features characterize an S_N1 transition state. Experimentally, primary ^{14}C KIEs have been measured as high as 1.160 for the S_N2 reaction of *N*,*N*-dimethyl-*p*-toluidine with benzyl(benzylsulfonate).[51] Effects similar to the primary

(40) Peng, C.; Schlegel, H. B. *Isr. J. Chem.* **1993**, *33*, 449−454.
(41) Anisimov, V.; Paneth, P. *J. Math. Chem.* **1999**, *26*, 75−86.
(42) Peng, C.; Ayala, P. Y.; Schlegel, H. B.; Frish, M. J. *J. Comput. Chem.* **1996**, *17*, 49.
(43) Northrop, D. B. *Annu. Rev. Biochem.* **1981**, *50*, 103−131.
(44) Parks, R. E.; Agarwal, R. P. In *The Enzymes*; Boyer, P. D., Ed.; Academic Press: New York, 1972; Vol. 7, pp 483−514.
(45) Rose, I. *Methods Enzymol.* **1980**, *64*, 47−59.
(46) Markham, G. D.; Parkin, D. W.; Mentch, F.; Schramm, V. L. *J. Biol. Chem.* **1987**, *262*, 5609−5615.
(47) Scheuring, J.; Berti, P. J.; Schramm, V. L. *Biochemistry* **1998**, *37*, 2748−2758.
(48) Rising, K. A.; Schramm, V. L. *J. Am. Chem. Soc.* **1997**, *119*, 27−37.
(49) Chen, X.-Y.; Berti, P. J.; Schramm, V. L. *J. Am. Chem. Soc.* **2000**, *122*, 6527−6534.
(50) Chen, C. Y.; Berti, P. J.; Schramm, V. *J. Am. Chem. Soc.* **2000**, *122*, 1609−1617.
(51) Yamataka, H.; Ando, T. *Tetrahedron Lett.* **1975**, 1059−1062.

^{14}C KIE of human TP, 1.139, have been measured in the reaction of pyridine with ^{14}C-methyl iodide (1.142)[52] and the attack of azide on benzyl chloride (1.130).[53] Although it has been suggested that an S_N2 KIE would be most fully developed when the leaving group and nucleophile are identical,[54] thereby increasing the symmetry of breaking and forming bonds, the above examples show that this is not necessarily the case. The 13.9% KIE of human TP is the largest primary ^{14}C KIE reported for an enzymatic reaction. For human TP, no oxacarbenium character is observed, and the large 1′-^{14}C KIE supports a symmetric transition state with similar bond order contributions from the attacking nucleophile and the leaving group.

It is worth noting that two independent groups have previously attempted to determine the transition state of TP using purely computational approaches.[55,56] Both of these studies come to the same conclusion: that TP catalyzes an S_N1 reaction. A computed TS structure, with no constraints, determined in this study also predicted an S_N1 TS (see Supporting Information). The KIEs calculated from a computed S_N1 TS differ substantially from those measured experimentally.

α-Secondary [1′-^{3}H]dT KIE. The inverse 1′-^{3}H KIE is consistent with an S_N2 reaction mechanism and suggests that the transition state is compressed slightly, with the nucleophile and/or leaving group sterically restricting the out-of-plane vibrational motion of H1′. α-Secondary ^{3}H KIEs are sensitive to changes in hybridization of the reactive carbon center to which they are bonded. A change from sp^3 to sp^2 hybridization will produce a large normal α-secondary ^{3}H KIE. These values are typically greater than 1.10 and theoretically can be as high as 1.58[54,57] for complete rehybridization at the transition state. In enzymatic systems, it is more common for α-secondary ^{3}H KIEs to be between 1.10 and 1.30 for S_N1 reactions, such as those for PNP (1.141), CTA (1.186), RTA (1.187), PTA (1.199), DTA (1.200), and uracil-DNA glycosylase (1.288). The α-secondary ^{3}H KIE for a symmetric S_N2 reaction should be unity because the reactive carbon undergoes no changes in hybridization during the reaction. Although inverse α-secondary ^{3}H KIEs can be indicative of hybridization change from sp^2 to sp^3, a small inverse α-secondary ^{3}H KIE, such as that observed in human TP, signifies a sterically crowed environment around the α-secondary ^{3}H, restricting the normal out-of-plane bending of the C−H bond. Typically, α-secondary ^{3}H KIE values for S_N2 reactions are between 0.91 and 1.08.[54]

***β*-Secondary proR and proS[2′-^{3}H] KIEs.** The measured KIEs for the 2′*R*-^{3}H and 2′*S*-^{3}H (−2.6 and 3.6%, respectively) are consistent with an S_N2 transition state. In S_N1 reactions for purine ribosides, the 2′ proton often exhibits a KIE of 10−15% due to hyperconjugative bond lengthening at C2′−H2′. An inverse effect from the 2′*R* position, while the 2′*S* KIE is small but normal, indicates that the transition state is compressed with respect to the 2′*R* position while shifting the 2′*S* proton into a conformation less vibrationally constrained than that of free substrate. The computationally predicted starting configuration of thymidine is 3′-*exo* and becomes more planar in the transition state. The product 2-deoxyribose 1-phosphate is predicted to have a 2′-*endo* configuration. Although hyperconjugation contributes significantly to the large normal 2′ proton KIE in the case of an oxacarbenium transition state, it plays little role in an S_N2 reaction where the bonding between C2′ and H2′ changes little in the transition state (Table 3).

Table 3. Bond Lengths and Bond Orders (in parentheses) for Substrate, Transition State, and Product

bond	reactant dT [Å(bond order[a])]	transition state [Å (bond order)]	2-dR1P [Å (bond order)]
C1′−N1	1.476 (0.980)	1.680 (0.497)	n.a.
C1′−O(P)	n.a.	1.760 (0.333)	1.395 (1.124)
C1′−H1′	1.096 (0.980)	1.105 (0.951)	1.090 (1.000)
C1′−C2′	1.535 (1.017)	1.549 (0.970)	1.527 (1.044)
C1′−O4′	1.413 (1.058)	1.405 (1.087)	1.444 (0.954)
C2′−H2′*R*	1.092 (0.993)	1.089 (1.003)	1.092 (0.993)
C2′−H2′*S*	1.091 (0.997)	1.097 (0.977)	1.096 (0.980)
C5′−H5′*R*	1.097 (0.977)	1.102 (0.961)	1.100 (0.967)
C5′−H5′*S*	1.095 (0.983)	1.099 (0.970)	1.103 (0.958)

[a] Bond orders are calculated using the equation $n_i = e^{(r_1 - r_i)/0.3}$, where n_i is the bond order, r_1 is the equilibrium bond length, and r_i is the nonequilibrium bond length. Equilibrium bond lengths used: C−N 1.47 Å, C−O 1.43 Å, C−H 1.09 Å, C−C 1.54 Å.

Remote [5′-^{3}H]dT KIE. The 5′-^{3}H KIE of 1.061 indicates polarization of the 5′ hydroxyl group or a 5′-OH dihedral to one of the 5′ C−H bonds that causes significant increase in that 5′ C−H bond length. On chemical grounds, there is no expectation of isotope effects four bonds distant from the reaction center. Despite this expectation, most *N*-ribosyl transferases give [5′-^{3}H] KIE of 3−5%. A remote KIE of 6.1% is exceptional among the growing family of these enzymes. Negative charge buildup on O5′ leads to loosening of the C−H bonds and could cause a normal KIE. For PNP, a 5′-^{3}H KIE of 1.033 was measured, and it was hypothesized that O5′ is in proximity to O4′, destabilizing the electrons on both oxygens and contributing to the formation of an oxacarbenium ion. This hypothesis was confirmed by the subsequent determination of the X-ray crystal structure of PNP with immucillin-H, a transition-state analogue, which showed O5′ located in an energetically unfavorable position close to O4′.[58] The other S_N1-type *N*-ribosyl transferases discussed above all have similar 5′-^{3}H KIEs. In TP, the nucleophilic transition state indicates no ribooxacarbenium ion character and suggests that an explanation must lie in 5′-OH H-bonding or the 5′-OH dihedral. Polarization of hydroxyl bonds not involved in the reaction can occur upon enzyme−substrate interaction. Changes between free thymidine and the transition state, including those in the Michaelis complex, are measured in *V*/*K* KIE experiments. According to the calculations of Lewis and Schramm[57] on glucose, this magnitude for the 5′-^{3}H KIE is easily achieved by a 2.6 Å H-bond between a negatively charged residue (Asp or Glu) and the hydroxyl in question. Even in the absence of any H-bond partner, a fixed dihedral angle between the 5′-pro*R* or *S* hydrogen and the 5′-OH bond of approximately 0°−25° or 100°−115° can induce an isotope effect of 1.06−1.08. Dihedral angles of 25°−100° or the presence of a H-bond increases the KIE even further. These effects are completely dependent on a preferred geometry at the catalytic site that differs from that in

(52) Bender, M. L.; Hoeg, D. F. *J. Am. Chem. Soc.* **1957**, *79*, 5649−5654.
(53) Raaen, V. F.; Juhlke, T.; Brown, F. J.; Collins, C. J. *J. Am. Chem. Soc.* **1974**, *96*, 5928−5930.
(54) Melander, L.; Saunders, W. H. *Reaction Rates of Isotopic Molecules*; Robert E. Krieger Publishing Company: Malabar, Florida, 1987.
(55) Cole, C.; Reigan, P.; Gbaj, A.; Edwards, P. N.; Douglas, K. T.; Stratford, I. J.; Freeman, S.; Jaffer, M. *J. Med. Chem.* **2003**, *46*, 207−209.
(56) Mendieta, J.; Martin-Santamaria, S.; Priego, E. M.; Balzarini, J.; Camarasa, M. J.; Perez-Perez, M. J.; Gago, F. *Biochemistry* **2004**, *43*, 405−414.
(57) Lewis, B. E.; Schramm, V. L. *J. Am. Chem. Soc.* **2003**, *125*, 4785−4798.
(58) Fedorov, A.; Shi, W.; Kicska, G.; Fedorov, E.; Tyler, P. C.; Furneaux, R. H.; Hanson, J. C.; Gainsford, G. J.; Larese, J. Z.; Schramm, V. L.; Almo, S. C. *Biochemistry* **2001**, *40*, 853−860.

solution. It is important to note that the nature of the TS is independent of the [5′-^{3}H] KIE since it is only used here as a remote label. Comparison of the [5′-^{3}H] and [5′-^{14}C] KIEs provides an internal control for the measurement since the carbon isotope effect is independent of geometry.[57]

Primary [1-^{15}N]dT KIE. The 1-^{15}N KIE reports the level of rehybridization of the pyrimidine nitrogen in the transition state with the maximum ^{15}N KIE predicted to be about 1.04 for full loss of a covalent bond. This intrinsic KIE of 1.022 indicates that there is significant loss of bond order to N1 of the thymine ring in the transition state. The computational model of the transition state that best matches the full family of KIEs gives a calculated 1-^{15}N KIE of 1.012, significantly smaller than the measured KIE of 1.022. The computed transition state does not include enzyme-induced changes in pyrimidine conjugation. The difference between intrinsic experimental and computational [1-^{15}N] KIE could be explained by the presence of polarizing groups adjacent to the pyrimidine ring carbonyl oxygens to withdraw electron density and reduce covalent bond order to N1. In the crystal structure of the *E. coli* TP with thymine, both an Arg and a Lys are within H-bond distance of the 4- and 2-carbonyl oxygens, respectively. These interactions suggest that the 2-carbonyl is H-bonded or transiently protonated at the transition state.

Comparison with Other Enzymatic S_N2 Displacements at Carbon. The KIEs measured for TP are similar to those observed with SAM synthetase where the 5′-^{14}C primary KIE is 1.128 and α-secondary 5′-^{3}H KIE is 1.000. In that reaction, the sulfur of methionine acts as a nucleophile, displacing the triphosphate from the 5′ carbon of ATP to form SAM. The transition state of SAM synthetase was determined to have 0.61 and 0.35 bond order to the nucleophile and leaving group, respectively. When the reduced mass for S and O are considered, these vibrational energies are approximately equivalent, making this a symmetric S_N2 transition state.[37] This transition state is similar to that determined here for TP (see Table 3) and provides another example of a strongly associative transition state characterized by a large primary ^{14}C KIE at the nucleophilic center. A similar example is provided by catechol *O*-methyl transferase where the nucleophilic oxygen from catechol displaces the *S*-adenosylhomocysteine of SAM to effect methylation of catechol. In this case, the ^{13}C KIE for the reaction center was 1.09, also interpreted as a symmetric nucleophilic displacement.[59]

Molecular Electrostatic Potential Comparison of Reactant and Transition State. For the purposes of TS characterization, the most important attributes are the nonequilibrium bond lengths of the forming and dissociating bonds and the overall electrostatic nature of the transition state. Changes in electrostatic potential for substrate, transition state, and product are shown in Figure 3. The transition state has continuous electron density extending from N1 through C1′ to the phosphate oxygen, as expected for an S_N2 transition state. The change in electrostatics upon conversion from substrate to transition state is less apparent than the change in geometry for the transition state. Transition-state analogues from enzymatic reactions are characterized by chemically stable analogues with appropriate bond lengths and charges. Since the transition-state ensemble involves pyrimidine, 2′-deoxyribose, and phosphate, mimics of this transition state will require chemically stable mimics of all three components.

Structural and Inhibitor Correlates with the Transition State for TP. The inhibitor 5-chloro-6-[1-(2-iminopyrrolidinyl)-methyl]uracil hydrochloride (TPI) has been proposed to be a transition-state analogue of TP, assuming that the transition-state structure is oxacarbenium-like and that the protonated pyrrolidine is an oxacarbenium mimic.[60] Computational analysis[55,56] predicted an S_N1 transition state for TP, based on the calculated charge distribution of TPI·HCl. Docking studies of protonated TPI into a homology model of human TP, based on the structure of *E. coli* TP, also predicted a dissociative oxacarbenium ion transition state. However, these models are based on the crystal structure of *E. coli* TP, solved to the relatively low resolution of 2.8 Å with thymine and sulfate bound in two separate structures. In these structures, the sulfate and thymine are bound too far apart (∼9 Å) for the reaction to occur, assuming both are bound in the appropriate cavity of the active site.[61] Thus, protein domain movement is necessary for catalysis. Conformational changes in enzymatic active sites are difficult to model without knowledge of both open and closed forms of the enzyme, and only the open form of TP has been reported. Human TP is approximately 39% identical in amino acid sequence to *E. coli* TP. Homology maps generated from sequences with identities below 50% can have significant rms deviations for the C_α backbone. Estimates are that 50% of all models generated from sequences of 40% identity will have C_α rms deviations of 2−3 Å.[62−66] One hypothesis concerning the relatively strong affinity of TP for TPI is that the positive charge buildup on the iminopyrolidine ring is acting not as a mimic of an oxacarbenium but as a phosphate "chelator", pulling the negatively charged phosphate close enough that the entire ion-pair complex begins to resemble the S_N2 transition state determined here. This hypothesis awaits structural confirmation.

The K_i of TPI is 20 nM,[67] to give a K_m/K_i value of 3000 for human TP. By comparison, the K_m/K_i value for DADMe-Immucillin-G, a transition-state analogue of human PNP, is 5 400 000.[68] Given the differences in structure between TPI and the transition state reported here, as well as the modest binding strength, it is apparent that TPI captures only a small fraction of the potential transition-state binding energy.

Comparison of Chemical and Enzymatic Transition States. Chemical solvolysis of thymidine might shed some light on this unprecedented S_N2 transition state for an *N*-ribosyl transferase. The pK_a of the 2-carbonyl oxygen of thymine is −2.98[69] which suggests that, at physiological pH, it is difficult to protonate this position to activate the leaving group. Such

(59) Heguzi, M. F.; Borehardt, R. T.; Schowen, R. L. *J. Am. Chem. Soc.* **1979**, *101*, 4359−4365.
(60) Price, M. L.; Guida, W. C.; Jackson, T. E.; Nydick, J. A.; Gladstone, P. L.; Juarez, J. C.; Donate, F.; Ternansky, R. J. *Bioorg. Med. Chem. Lett.* **2003**, *13*, 107−110.
(61) Walter, M. R.; Cook, W. J.; Cole, L. B.; Short, S. A.; Koszalka, G. W.; Krenitsky, T. A.; Ealick, S. E. *J. Biol. Chem.* **1990**, *265*, 14016−14022.
(62) Reliability of models generate by SWISS-MODEL. http://www.expasy.org/swissmod/SM_likelyprecision.html.
(63) Chothia, C.; Lesk, A. M. *EMBO J.* **1986**, *5*, 823−826.
(64) Harrison, R. W.; Chatterjee, D.; Weber, I. T. *Proteins: Struct., Funct., Genet.* **1995**, *23*, 463−471.
(65) Guex, N.; Peitsch, M. C. *Electrophoresis* **1997**, *18*, 2714−2723.
(66) Bajorath, J.; Stenkamp, R.; Aruffo, A. *Protein Sci.* **1993**, 2.
(67) Uracil derivatives and antitumor effect potentiator and antitumor agent containing the same. U.S. Patent 5,744,475, April 28, 1998.
(68) Basso, L. A.; Santos, D. S.; Shi, W.; Furneaux, R. H.; Tyler, P. C.; Schramm, V. L.; Blanchard, J. S. *Biochemistry* **2001**, *40*, 8196−8203.
(69) Poulter, C. D.; Fredrick, G. D. *Tetrahedron Lett.* **1975**, *26*, 2171.

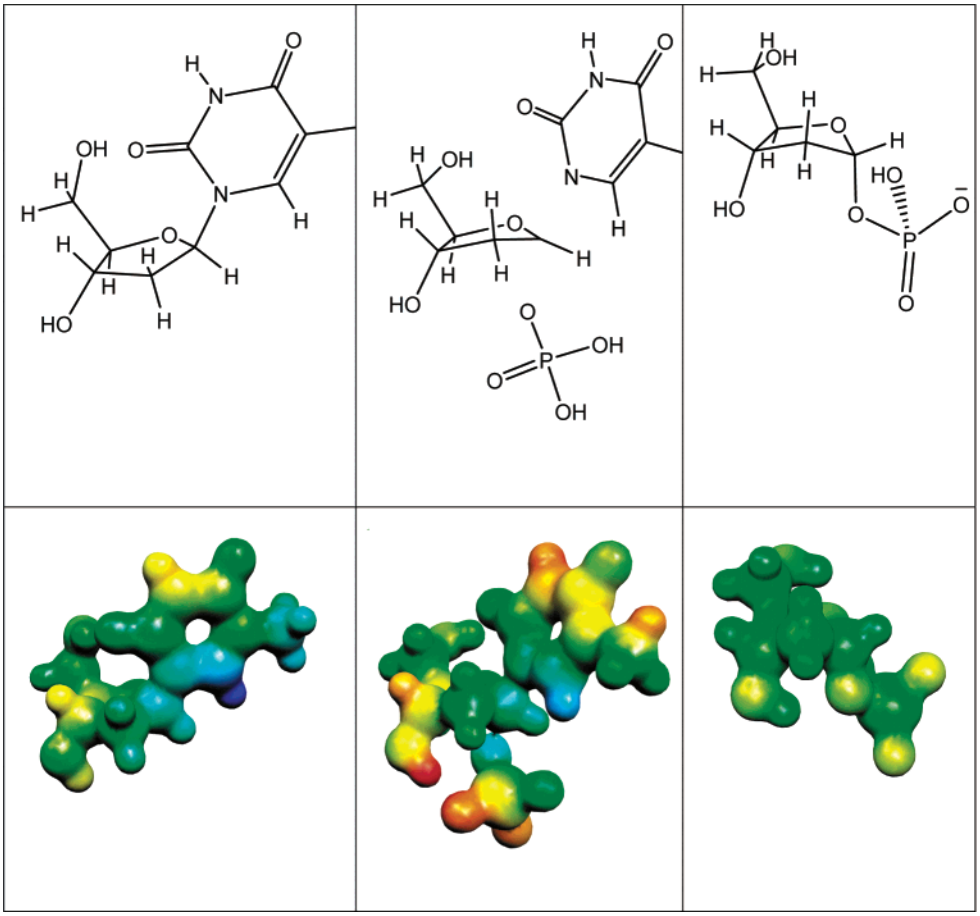

Figure 3. Substrate, transition state, and product of human TP as modeled in the gas phase at B1LYP/6-31G*. In the upper panels, methyl protons and orientation of O−H bonds have been eliminated for clarity. The lower panels represent the electrostatic potentials of those structures displayed in the upper panels. Red represents negative potential, blue represents positive, and green is neutral. Electrostatic potential maps in the lower row are in the same orientation as the structures shown in the upper. The surfaces shown are at 0.2 mb/Å^2 to provide clear atomic outlines.

leaving group activation is seen in PNP, where N7 of inosine (pK_a = 1.2)[70] becomes protonated at the transition state, significantly assisting leaving group dissociation without nucleophilic participation. In TP, this sort of leaving group activation is not likely, requiring a higher degree of nucleophile participation for the reaction to proceed. This inherently reduced reactivity may also help to explain the slower catalytic rate of TP compared to PNP (2 s^{-1} vs 12 s^{-1}). Uracil-DNA glycosylase may prove to be unique among the pyrimidine ribosyltransferases, with the observed S_N1 mechanism due mainly to neighboring group participation in a polynucleotide context.

Conclusions

The nucleophilic transition state observed in human TP is the first case of an S_N2-type reaction for the family of *N*-ribosyl transferases. Comparing the transition-state structure reported here with compounds currently being developed as putative transition-state analogues readily explains the modest affinity of current TP inhibitors. The assumption that the transition state of TP resembles that of purine *N*-ribosyl transferases is incorrect. Transition state analogues designed to bind tightly to TP must therefore mimic this S_N2 transition state. Knowledge of the transition-state structure for TP may enable the design of more potent inhibitors of human TP. These are important for the eventual development of effective chemotherapeutics for use in the treatment of solid tumors.

Acknowledgment. The authors thank Drs. Richard H. Furneaux and Peter C. Tyler of Industrial Research, Ltd. (Lower Hutt, NZ) for the synthesis of [1-^{15}N]thymine, Prof. Joanne Stubbe (Massachusetts Institute of Technology) for the generous gift of the plasmid expressing ribonucleotide triphosphate reductase, Mr. Edward Nieves for assistance with mass-spectrometry, and Dr. Paula Krosky of the National Institutes of Health for production of recombinant human TP. This work was supported by research grants from the National Institutes of Health, a RAND grant from the National Cancer Institute, and an Einstein Postdoctoral Scholar Award.

Supporting Information Available: The supplement documents features of the calculated TS, along with frequency tables and, where appropriate, calculated KIEs (PDF). This material is available free of charge via the Internet at http://pubs.acs.org.

JA039260H

(70) Dawson, R. M. C.; Elliott, D. C.; Elliott, W. H.; Jones, K. M. *Data for Biochemical Research*, 3rd ed.; Clarendon Press: Oxford, UK, 1986.